DOI: 10.1002/chem.200801521

Chemoselective Capture of Glycans for Analysis on Gold Nanoparticles: Carbohydrate Oxime Tautomers Provide Functional Recognition by Proteins

Mikkel B. Thygesen, Jørgen Sauer, and Knud J. Jensen*[a]

Abstract: Nanoparticles functionalized with glycans are emerging as powerful solid-phase chemical tools for the study of protein–carbohydrate interactions using nanoscale properties for detection of binding events. Methods or reagents that enable the assembly of glyconanoparticles from unprotected glycans in two consecutive chemoselective steps with meaningful display of the glycan are highly desirable. Here, we describe a novel bifunctional reagent that 1) couples to glycans by oxime formation in solution, 2) aids in purification through a lipophilic trityl tag, and 3) after deprotection then couples to gold nanoparticles through a thiol. NMR studies revealed that these oximes exist as both the open-chain and *N*-glycosyl oxy-amine tautomers. Glycan-linker conjugates were coupled through displacement of ligands from preformed, citrate-stabilized gold nanoparticles. Recognition of these glycans by proteins was studied with a lectin, concanavalin A (ConA), in an aggregation assay and with a processing enzyme and glucoamylase (GA). We demonstrate that the presence of the *N*-glycosyl oxy-amines clearly enables functional recognition in sharp contrast to the corresponding reduced oxy-amines. This concept is then realized in a novel reagent, which should facilitate nanoglycobiology by enabling the operationally simple capture of glycans and their biologically meaningful display.

Keywords: glycoconjugates · gold · molecular recognition · nanotechnology · proteins

Introduction

Glycans are central to many fundamental biological processes, such as, cell–cell recognition, detection, and evasion, raising of immune responses, cell attachment, cell fate, development, and morphogenesis.[1–3] Solid-phase chemical methods are gaining importance as a tool enabling the study of these processes.[4]

Chemoselective coupling of unprotected carbohydrates to, for example, polymeric supports,[5–7] microarrays,[8–10] peptides and proteins,[11] and to other surfaces[12] through oxime formation has been widely exploited in recent years as a means to capture glycans from natural sources and to obviate laborious glycosylation and protecting-group chemistry. The reaction exploits the unique availability of an aldehyde moiety in the reducing-end of glycans, which also allows, for example, reductive amination, hydrazone and acyl hydrazone formation, and thiazolidine formation.[13] With the recent advances in the preparation of complex oligosaccharides of biological relevance through chemical and chemoenzymatic methods,[14] researchers have increasing access to glycans in low quantities related to, for example, studies on signaling, pathogenic and viral infections, fertility, immunity, and cancer.[15] The development of tools for the study of these interactions, providing functional recognition of carbohydrates by proteins and other biomolecules, constitutes an important basis for glycobiology and glycomics, that is, the high-throughput study of the biological roles of carbohydrates in living organisms.

A central solid-phase chemical tool is represented by glyconanoparticles, which have recently attracted attention as probes for the study of carbohydrate–protein and carbohydrate–carbohydrate interactions.[4,16] These metal and semiconductor nanoparticles covered with monolayers of carbohydrates offer some unique advantages over other multivalent carbohydrate-functionalized structures (e.g., dendrimers, polymers, liposomes) in the combined properties of the clustered multivalent presentation of the carbohydrates on the surface, the possibility for facile tracing by means of electron microscopy, light scattering, or fluorescence emission, the relatively small size that allows in vivo bio-imaging,

[a] M. B. Thygesen, Dr. J. Sauer, Prof. K. J. Jensen
Department of Natural Sciences, Faculty of Life Sciences
Centre for Carbohydrate Recognition and Signalling
University of Copenhagen, Thorvaldsensvej 40
1871 Frederiksberg (Denmark)
Fax: (+45) 353-32-398
E-mail: kjj@life.ku.dk

Supporting information for this article is available on the WWW under http://dx.doi.org/10.1002/chem.200801521.

and the high degree of solubility and stability in buffered aqueous media. The three-dimensional presentation on the spherical nanoparticles results in a flexible globular shape that can be thought of as a model for the glycocalyx of cell surfaces.[17] Of particular importance are the optical properties of gold nanoparticles (AuNPs), notably the changes in surface-plasmon resonance upon association, which have been exploited in applications of gold glyconanoparticles (glyco-AuNPs) for the in vitro detection of, for example, carbohydrate–protein interactions. The rapid developments in this field have to a great extent been fueled by the introduction of the Brust–Schiffrin two-phase protocol for the preparation of functionalized AuNPs,[18] in which ligand-capped AuNPs are produced in a *one-step* approach. Alternative methods for AuNP preparation have been available for several decades, for example, the methods of Turkevich[19] and Frens,[20] in which a two-step procedure is typically used, that is, AuNP preparation followed by the introduction of the desired ligands. The highly polar ligand shell of glyco-AuNPs represents a challenge to AuNP preparation by the Brust–Schiffrin protocol due to the incompatibility of the polar shell with organic solvents. In typical modifications of the procedure, the AuNPs are prepared in polar organic solvents such as methanol in a homogenous phase.[21] A considerable limitation of these *one-step* procedures for comparative (parallel) studies is the high degree of dependency of particle growth on the nature of the thiol ligands.[17,22,23] This may be circumvented by use of two-step procedures, in which the initial preparation of the AuNP cores is followed by introduction of carbohydrate ligands, hereby allowing the use of single batches of AuNPs for multiple ligands.[24] Both types of procedure, however, require access to thiol-functionalized glycans.

Attachment of carbohydrates to AuNPs through thiol-containing linkers has been performed typically by extensive protecting-group and glycosylation chemistry in solution. This approach for the preparation of glyconanoparticles was introduced by Penadés and co-workers[17,21] to present glucose, lactose, maltose, and the Lewis^x trisaccharide on AuNPs. A similar approach has been taken by the groups of Russell,[24] Lin,[25] Barchi,[26] and others.

Reductive amination chemistry for glyco-AuNP preparation was introduced by Kamerling and co-workers for the thiol-functionalization of unprotected glycans.[22] In this procedure, the classical method of conversion of the reducing-end saccharide unit into an open-chain secondary amine by reduction was used.[27] However, the lack of specific binding between proteins and glycans attached by means of reductive amination was highlighted recently by Feizi and co-workers.[10] Here, lectin and antibody affinity for short glycans, for example, Le^a and Le^x trisaccharides, was shown to be dependent on the presence of an unmodified (i.e., pyranose) core-monosaccharide unit. Glycans attached through oxime formation could be recognized, whereas reductive amination resulted in complete loss of affinity, demonstrating that at least for some carbohydrate–protein interactions, the ring-closed form (i.e., the *N*-glycoside) of the carbohydrate oximes appears to be recognized. Shin and co-workers have reported interactions of cyclic tautomer forms of carbohydrate acylhydrazones with proteins.[8] Additionally, *N*-methyl substituted aminooxy derivatives have been pursued.[9,28]

Carbohydrate oximes and oxime ethers are known to exist in several ring-chain tautomeric forms,[29] of which the open-chain *E* and *Z* forms generally predominate over the pyranose β and α forms,[30–32] as shown for D-glucose in Scheme 1. Additionally, furanose β and α forms may constitute minor tautomers (not shown). Isomerization of the open-chain oximes is mediated by the closed forms. However, the distribution of tautomer forms is dependent on the monosaccharide unit.

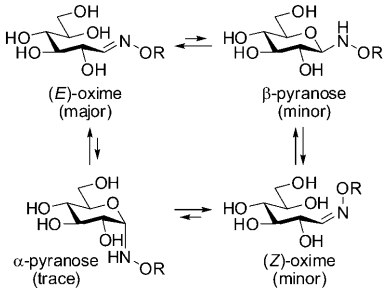

Scheme 1. Ring-chain tautomers of glucose oxime ethers. Adapted from ref. [30].

In this paper, we describe the use of carbohydrate oxime formation for the attachment of glycans to gold nanoparticles. To our knowledge, this is the first example of such use. Moreover, we study the consequences of tautomerism of carbohydrate oxime ethers during interaction with proteins by comparing the functional binding of oxime ring-chain tautomers with analogues "locked" in an open-chain configuration by reduction of the oximes to hydroxylamines. For this purpose, we chose the hydrolytic enzyme glucoamylase (GA) from *Aspergillus niger* and the lectin concanavalin A (ConA) from *Concanavalia ensiformis*.

Results and Discussion

The linker moiety between glycan and nanoparticle is of crucial importance for interactions of glyco-AuNPs with proteins. The length and nature of the linker between the reducing end of the saccharide and the mercapto group (for attachment to the gold surface by formation of a covalent Au–S bond) affects the ligand density, but may also play a role in the organization of the monolayer and on the solubility and bio-compatibility of the resulting nanoparticles. The use of well-defined poly(ethylene glycol) (PEG) polymers and monodisperse oligo(ethylene glycol)s (OEGs) has emerged as a means to improve biological and pharmaceutical properties of, for example, proteins[33] and drug molecules[34] and these are also widely used as linkers for surfaces including nanoparticles. Among the reported effects of

PEGs and OEGs are, for example, prevention of degradation by hydrolytic and proteolytic enzymes, shielding of antigenic or immunogenic epitopes, improvement of aqueous solubility, reduction of non-specific binding, and prolongation of systemic circulation.[33,34]

Alkanethiolate-linked OEGs, that is, $R(CH_2CH_2O)_n(CH_2)_mSH$ with n typically around 4 and m around 11, introduced by Whitesides and co-workers,[35] have been used on gold nanoparticles to produce aqueously soluble particles with increased non-specific protein resistance.[36,37] Alternatively, the aliphatic chain may be omitted with similiar results by the use of thiol-terminated OEGs, that is, $RCH_2CH_2(OCH_2CH_2)_nSH$ with n typically around 4, which are more easily obtained.[38–41] The differences in the assembly and ordering of monolayers between these two types of OEG ligands are not clearly understood, however, the OEG section of the monolayers is generally believed to contain more random orientations of individual chains than the close packing of alkanethiolate monolayers.[39,42]

The optimal length of OEG linkers for bioanalytical assays is a compromise between several factors, such as the flexibility and accessibility of the ligands, the solubility and stability of the glyco-AuNPs, and a maximum assay response, for example, in surface-plasmon-resonance measurements by using UV-visible light. Short linkers may provide an increased assay sensitivity[24] but may also lead to poor solubility.[22] Additionally, Li and Peng have shown that the photochemical stability of AuNPs is dependent on the length of the linker;[43] long alkanethiolate linkers provide improved stability over shorter linkers. In light of these considerations, we chose to work with OEG linkers consisting of thiol-terminated tetra(ethylene glycol).

We have designed and synthesized a novel OEG linker that allows two sequential highly chemoselective reactions: 1) attachment of a glycan to the linker via carbohydrate oxime formation, and 2) anchoring of the linker to the particle surface. The linker incorporates a removable trityl moiety to aid in isolation of the glycan-linker conjugates. This approach provides easy-to-handle yet efficient coupling of biomolecules to nanoparticles to generate functionalized nanoparticles for bioanalytical assays.

Preparation of OEG glycoconjugates: Mitsunobu chemistry was used to introduce *N*-hydroxyphthalimide (PhthN-OH) on tetra(ethylene glycol), see Scheme 2. The de-symmetrization of the OEG was performed with stoichiometric amounts of the nucleophile, thus the theoretical yield would be 50%. Examination of the reaction mixture indicated complete consumption of *N*-hydroxyphthalimide and a **1**/**bis-1** ratio of 2:1 as expected, however, the isolated yield of **1** was 37% (74% when corrected for statistical distribution). Recovery of the bis-substituted product (**bis-1**) provided a yield of 18%, indicating that product was lost during the purification step, possibly by covalent attachment to silica; we note that, contrary to *N*-alkylphthalimides, the *N*-alkoxyphthalimide moiety is highly reactive and that addition of alcohols such as methanol to solutions of **1** result in partial ring

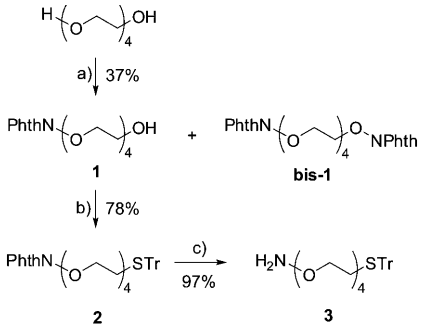

Scheme 2. Preparation of heterobifunctional aminooxy linker **3** from tetra(ethylene glycol). a) 1 equiv PhthN-OH, PS-PPh_3, diisopropyl diazodicarboxylate (DIAD), 16 h; b) TrSH, PS-PPh_3, DIAD, 0°C→RT, 16 h; c) hydrazine hydrate, MeCN, RT, 2 h.

opening and formation of mixed hydroxamic/carboxylic esters (data not shown). Following the isolation of **1**, a second Mitsunobu reaction was performed with triphenylmethanethiol to obtain the orthogonally protected heterobifunctional linker **2** in 78% yield. The Mitsunobu reaction with triphenylmethanethiol, reported initially by Jin et al.[44] in 2005, is a highly convenient method for the "thiolation" of OEGs that obviates the use of volatile sulfur compounds typically used in alkylation protocols. Purification of **1** and **2** was simplified by the use of polymer-supported triphenylphosphine that could be removed by simple filtration.

Removal of the labile Phth-protecting group from heterobifunctional linker **2** with hydrazine hydrate at room temperature provided cleanly the aminooxy linker **3**, which was coupled to glucose, maltose, and maltotriose by treatment with unprotected glycans under mildly acidic conditions. The resulting carbohydrate oxime ethers **4**–**6** were isolated in good yields (74–88%, Scheme 3). A key feature of the design of linker **3** is that upon formation of glycan-linker conjugates, it allows easy detection and isolation on silica gel or by reverse-phase chromatography (HPLC or solid-phase extraction, SPE) due to the presence of the lipophilic and UV-active trityl group.

NMR analyses of compounds **4**–**6** in [D_4]methanol allowed the identification of (*E*)- and (*Z*)-oxime tautomers as well as the cyclic ring-chain tautomers as minor constituents. HSQC data showed that the cyclic ring-chain tautomers had $J_{H1,H2}$ coupling constants in the range 9.1–9.2 Hz, thus indicating that they were in the β-pyranose configuration. The estimated (*E*)-oxime/(*Z*)-oxime/β-pyranose ring-chain tautomer ratio of 60:20:20 was identical for compounds **4**–**6**. Diagnostic NMR signals for glucose oxime **4** tautomers are provided in Table 1. These assignments were nearly identical for maltose and maltotriose oximes **5** and **6** (see Experimental Section).

An investigation of the possible pH dependency of the ring-chain tautomeric equilibrium was conducted with a ^{13}C-labeled analogue of **4**, prepared from D-[1-^{13}C]glucose and **3**. In [D_4]methanol, this compound (**16**) had an (*E*)-oxime/(*Z*)-oxime/β-pyranose ring-chain tautomer ratio of 60:20:20. The pH of the solution ([D_4]methanol/H_2O 4:6) was controlled

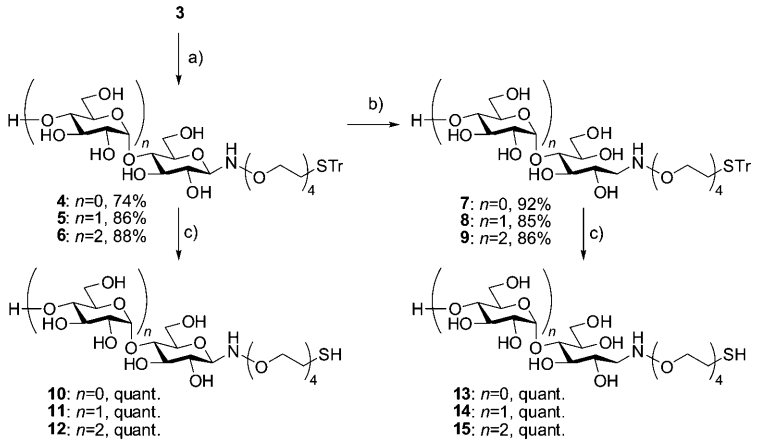

Scheme 3. Preparation of OEG glycoconjugates **4–6** by oxime coupling and subsequent reduction to oxy-amines **7–9**. Removal of the trityl groups furnished thiol glycoconjugates **10–15** for coupling with gold nanoparticles. Carbohydrate oximes are depicted as the β-pyranose tautomer for the sake of clarity (Scheme 1). a) Glucose/maltose/maltotriose (1.1 equiv), MeCN, H_2O, HOAc, 16 h; b) $NaBH_3CN$ (2 equiv), HOAc, 2 h; c) TFA, triethylsilane (TES), CH_2Cl_2, 5 min.

Table 1. Diagnostic NMR signals of tautomers of glucose oxime **4**.

Tautomer[a]	H1[b]/C1 [ppm]	H2/C2 [ppm]	H3/C3 [ppm]
(*E*)-oxime	7.44 (6.7)/151.8	4.32/72.2	3.86/72.6
(*Z*)-oxime	6.78 (6.0)/154.2	4.94/68.6	3.90/74.9
β-pyranose	4.11 (9.2)/92.9	3.20/79.2	N.A.

[a] See Scheme 1. [b] Values in parenthesis denote $J_{H1,H2}$ coupling constants in Hz.

by acetate buffering at pH 7, 6, 5, 4, 3, and 2, and the relative ratio of ring-chain tautomers was monitored by recording the anomeric signals in ^{13}C NMR spectroscopy (see Supporting Information). We found that the tautomer ratio was essentially identical down to pH 2. A related study on carbohydrate acetylhydrazones has indicated a similar reduced basicity of the anomeric nitrogen.[45]

The carbohydrate oximes **4–6** were reduced by treatment with sodium cyanoborohydride employing acetic acid as the solvent. The resulting oxy-amines **7–9** were isolated by ion-exchange chromatography (SPE cartridges) in high yields (85–92%, Scheme 3). NMR spectroscopy confirmed the conversion of all ring-chain tautomers of **4–6** into single species for **7–9**.

Functional recognition of oxime tautomers of OEG glycoconjugates by glucoamylase: An assay based on glucoamylase (GA; 1,4-α-D-glucan glucohydrolase, EC 3.2.1.3) from *Aspergillus niger* was selected for assessment of the functional recognition of OEG glycoconjugates **4–9** by hydrolytic enzymes. GA catalyzes the hydrolysis of α-1,4 and to a lesser extent α-1,6 glucosidic linkages from the non-reducing end of starch and related glycans to release D-glucose.[46–49] The active site of GA contains two glutamic acids positioned at positions 179 and 400 of the protein sequence acting as a general acid catalyst and base, respectively.[50,51] The hydrolysis of substrate is accomplished by the donation of a proton from Glu179 to the scissile glycosidic bond and a nucleophilic attack by water on C-1 in the transition-state oxocarbenium ion, catalyzed by Glu400.[52–57] The two catalytic residues protrude in the bottom of a funnel-shaped passage created by six highly conserved regions that constitute the GA-characteristic $(\alpha/\alpha)_6$-barrel domain.[52,54,55,58] These α-helical segments form the major part of an active-site pocket that is believed to contain seven subsites that can accommodate *one* glycosyl residue each.[59–61] The hydrolytic event occurs between subsites −1 and 1 and requires the substrate to bind in a productive mode in these two terminal sites, thereby exposing the glycosidic linkage to the catalytic residues. The affinities of subsites −1 and 1 estimated from pre-steady-state association constants indicates that the initial binding of substrate is controlled by a very high affinity in subsite −1 with subsite 1 having much lower affinity.[62] A combination of site-directed mutagenesis, different dissacharide substrates, and inhibitors have been used for mapping the affinity of these two subsites and their role in hydrolysis.[52,54,63–66] One of these inhibitors/substrates is maltitol (4-*O*-α-D-glucopyranosyl-D-glucitol), the reduced form of maltose, that is hydrolyzed only slowly by GA despite the fact that the α-1,4-glycosidic bond is retained after reduction of maltose. A possible explanation for this has been suggested by Günther and Heymann in a study of subsites in pig intestinal glucoamylase–maltase complex[67] based on the reaction mechanism originally proposed for glycosidases.[68] According to this model, the reaction rate depends on the optimal orientation of the glycosidic oxygen atom relative to the active-site acidic residue. The orientation of this atom is a function of the glycosidic bond and the 'aglycon' residue. Thus, for optimal hydrolysis, a glycosidic α-1,4 configuration and an 'aglycon' glucopyranosyl ring structure is necessary. In substrates with other geometric configurations, for example, open-chain, the initial protonation of the glycosidic oxygen by the catalytic acid is less favorable.

We hypothesized that the ring-chain tautomeric equilibrium of **4–6** would result in functional recognition of the reducing-end residue, which would not be possible with the open-chain configuration in **6–9**. Indeed, incubation with GA in 50 mM acetate buffer pH 4.5 at 42 °C for 20 h followed by HPLC analysis showed full conversion of both **5** and **6** into **4**, that is, one glucose unit was cleaved from the maltose oxime and two glucose units were cleaved from the maltotriose oxime. For carbohydrate oxy-amines **6–9**, however, **9** was converted into **8** as expected, that is, one glucose

unit was cleaved from the maltotriose oxy-amine, but there was only minor conversion of **8** and **9** to **7**, that is, the maltose oxy-amine was not a good substrate for GA (Figure 1). This result is in agreement with the different substrate specificities of GA towards maltose and maltitol, as described above. This leads to the very important conclusion that the carbohydrate oxime allows functional recognition by glucoamylase of ring-closed (*N*-glycosyl oxy-amine) tautomers.

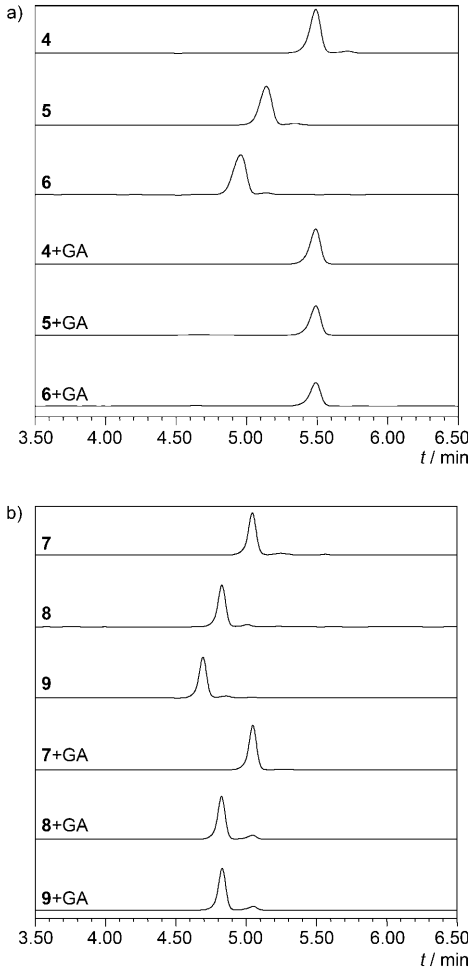

Figure 1. HPLC chromatograms (215 nm) of OEG glycoconjugates before (top three rows) and after (bottom three rows) incubation with glucoamylase (+GA) in 50 mM sodium acetate buffer pH 4.5 at 42 °C for 20 h. a) Oximes **4**–**6**; b) Oxy-amines **7**–**9**.

Next, we applied a quantitative colorimetric assay based on the coupling of the GA assay with a glucose oxidase/peroxidase assay. If performed in acetate buffer pH 4.5 at 42 °C for 20 h, incubation of the glucose oxime **4** showed a small signal, indicative of partial hydrolysis (<10%) of the oxime bond under these assay conditions. Accordingly, we changed the assay conditions to 10 mM phosphate buffer pH 7.0 at 42 °C for 20 h, which resulted in a drastic reduction of non-enzymatic oxime hydrolysis of **4**–**6**, however, we note that pH 7 is suboptimal for glucoamylase.[52] The glucoamylase–glucose oxidase/peroxidase assay was conducted on a 10-nmol-substrate scale (Table 2). These results clearly demonstrate that for carbohydrate oximes **4**–**6** the maltose and maltotriose derivatives are hydrolyzed to the glucose stage, whereas for carbohydrate oxy-amines **7**–**9** (locked open-chain) only the maltotriose derivative is a substrate for GA and that hydrolysis stops at the maltose stage.

As a control experiment, we wanted to study whether the enzymatic cleavage of **5** to **4** by GA could occur by means of an unexpected oxime cleavage in acetate buffer. Specifically, we wanted to study, and exclude, the possibility that hydrolysis of **5** to **4** proceeded by means of 1) oxime hydrolysis, followed by 2) cleavage of maltose in solution, and finally by 3) reformation of the oxime between glucose and linker **3**. Two exchange studies were performed in 50 mM acetate buffer pH 4.5 at 42 °C for 20 h in which 1) **5** was incubated with an equimolar amount of glucose in the absence of GA, and 2) **4** was incubated with an equimolar amount of [1-^{13}C]glucose in the presence of GA. Analysis by mass spectrometry showed the *absence* of the putative exchange product in both cases. These results strongly demonstrated that under these conditions, the oxime linkage remained stable and that the glycan of oxime **5** was recognized by GA, most likely as the ring-closed, *N*-glycosidic tautomer.

Preparation of glyconanoparticles: OEG glycoconjugates **4**–**9** were deprotected by treatment with trifluoroacetic acid under anhydrous conditions and in the presence of triethylsilane as a scavenger to furnish the thiols **10**–**15** in quantitative yields (Scheme 3). Variable amounts (0–40%) of the corresponding disulfides were observed by NMR spectroscopy.

Citrate-capped gold nanoparticles were prepared according to a modification[69] of the Turkevich protocol[19] to provide spherical AuNPs with an average diameter of 12 nm and a concentration of 18 nM, as determined by transmission electron microscopy (TEM) and UV-visible spectroscopy.[70]

The glycan-linker conjugates **10**–**15** were anchored to the AuNPs through displacement of the citrate by stirring in aqueous media for a minimum of 16 h (Scheme 4). Gold glyconanoparticles (**10-AuNP** to **15-AuNP**) were purified by repetitive (5×) centrifugal filtration (50 kDa cut-off) of aqueous washings, and redissolved to final concentrations of 0.50 μM in 10 mM phosphate buffer pH 7.0. A slight red-shift of ≈4 nm was observed in the UV-visible spectrum upon coating with thiols **10**–**15**. All glyconanoparticles had a surface-plasmon-resonance peak maximum at 523 nm in aqueous media, and solutions were stable for at least six months, as witnessed by the lack of changes in their UV-visible spectra during this period. Analysis by TEM confirmed that there were no changes in AuNP diameter upon treatment with the thiol-containing glycoconjugates (Supporting Information).

Glyconanoparticles **10-AuNP** to **15-AuNP** were freely soluble in 10 mM phosphate buffer at pH 7.0, however, rapid aggregation of **13-AuNP**, **14-AuNP**, and **15-AuNP**, which contained the reduced oximes, was observed in 50 mM acetate buffer at pH 4.5. On the other hand, under these condi-

Table 2. Quantitative measurements of release of glucose from free and captured glycans (**4**–**9**) by glucoamylase.[a]

Glycan	Glucose			Maltose			Maltotriose		
	unmodified	oxime (**4**)	oxy-amine (**7**)	unmodified	oxime (**5**)	oxy-amine (**8**)	unmodified	oxime (**6**)	oxy-amine (**9**)
released glucose [nmol]	9.14 ± 0.6	0.17 ± 0.08	0.16 ± 0.07	19.73 ± 0.2	8.00 ± 0.3	0.72 ± 0.2	30.11 ± 1.5	17.99 ± 0.4	8.73 ± 0.4

[a] Hydrolysis was performed in 10 mM sodium phosphate pH 7.0 at 42 °C using 10 nmol of each compound. The exact points of hydrolysis are illustrated on the graphics by dashed lines. Carbohydrate oximes are depicted as the β-pyranose tautomer for the sake of clarity (Scheme 1).

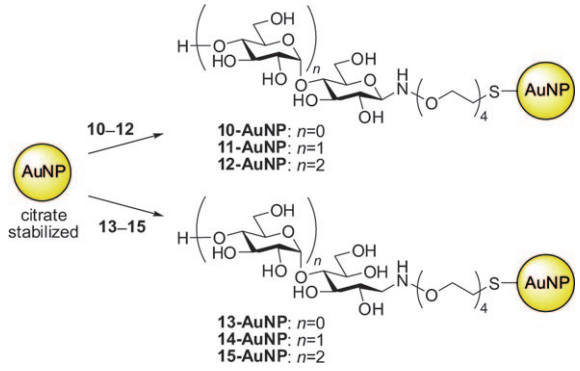

Scheme 4. Preparation of glyconanoparticles **10-AuNP** to **15-AuNP**. Carbohydrate oximes are depicted as the β-pyranose tautomer for the sake of clarity (Scheme 1).

tions **10-AuNP**, **11-AuNP**, and **12-AuNP**, containing carbohydrate oximes, remained freely soluble. We attribute this effect to protonation of the oxy-amines in **13-AuNP**, **14-AuNP**, and **15-AuNP**, the pK_a values of which are expected to be in the 4–5 range (based on the pK_a of *N*,*O*-dimethyl hydroxylamine of 4.75[71]). We speculate that electrostatic interactions between protonated oxy-amines and negative charges associated with the gold surface led to the observed aggregation under acidic conditions.

Biological recognition of oxime tautomers on glyco-AuNPs by the lectin concanavalin A: With the novel glyconanoparticles at hand, we sought to establish whether the ring-chain tautomerism of the carbohydrate oximes would have an impact on the binding to carbohydrate-binding proteins. For this purpose we chose the lectin concanavalin A (ConA) from *Canavalia ensiformis*. This lectin has an affinity for terminal α-D-glucopyranose residues as well as for α-D-mannopyranose residues, and interactions of this lectin with glyconanoparticles have been studied by several groups.[22,24,25] Comparison of relative binding affinities of methyl α-glucoside, maltose, maltitol, and maltotriose in the literature[72,73] show that these glycans bind to ConA with identical affinity in the low-millimolar range, consistent with a single-residue binding site,[74] whereas the affinity of β-glucosides is lowered by an order of magnitude.

Glyconanoparticles (5 nM) containing maltotriose as the oxime and oxy-amine (**12-AuNP** and **15-AuNP**, respectively), as well as glucose as the oxime and oxy-amine (**10-AuNP** and **13-AuNP**, respectively) were subjected to a ConA concentration of 5 μM, and lectin-mediated glyconanoparticle aggregation was observed as a shift in the surface-plasmon band that could be measured spectrophotometrically (Figure 2). Our results clearly show that both maltotriose-containing AuNPs underwent extensive lectin-mediated aggregation, but more importantly, that unlike the lectin-induced aggregation with the glucose oxime AuNPs (**10-AuNP**), the glucose oxy-amine AuNPs (**13-AuNP**) displayed a complete lack of surface-plasmon band shift upon addition of the lectin. We rationalize this striking difference in lectin-induced aggregation as a consequence of the different glucose structures presented to the lectin by **10-AuNP** and **13-AuNP**: the former, which includes a ring-closed, *N*-glycosidic tautomer, could be recognized by ConA, whereas the latter, with its acyclic, open-chain form, could not. This result also shows that the specificity of the lectin binding

plays the dominant role and that unspecific protein interactions are minimal.

At lower ConA concentration (1 μM), the glucose oxime AuNPs (**10-AuNP**, ring-form predominantly β-pyranoside) displayed less of a shift of the surface-plasmon band than seen for **11-AuNP** and **12-AuNP** (Supporting Information), consistent with the higher binding of α-glucosides, as described above. Control experiments with bovine serum albumin (BSA) at 5 μM showed complete absence of a surface-plasmon band shift with all glyconanoparticles (**10-AuNP** through **15-AuNP**) throughout the 48 h period (see Supporting Information for **10-AuNP**), confirming the insignificance of non-specific interactions and the specificity of the glyconanoparticle–lectin recognitions.

It seems from the results in Figure 2 that the onset of aggregation was slower for the maltotriose oxy-amine AuNPs (**15-AuNP**) than for the corresponding oxime AuNPs (**12-AuNP**). This effect, given the identical nanoparticle size of the two samples and supposing identical binding affinities of the individual maltotriose conjugates for ConA, could be related to a difference in ligand density of these glyco-AuNPs.

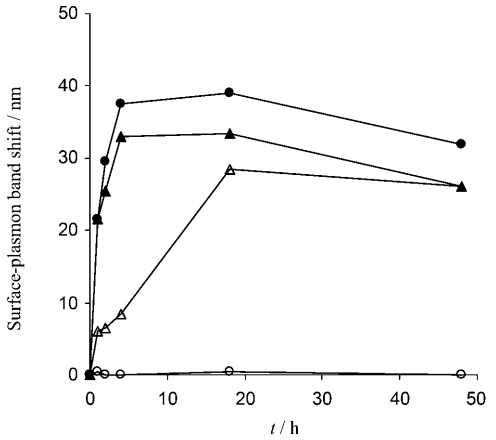

Figure 2. Lectin-induced nanoparticle aggregation as monitored by a shift in surface-plasmon band maximum for glyco-AuNPs **10-AuNP** (●), **12-AuNP** (▲), **13-AuNP** (○), and **15-AuNP** (△) upon addition of 5-μM concanavalin A.

Determination of ligand density of glyco-AuNPs by glucoamylase and thiolytic release: To estimate the ligand density of the prepared glyconanoparticles, we performed a series of thiolytic-release (ligand-displacement) experiments on the glyconanoparticles. Glyconanoparticles were exposed to excess 2-mercaptoethanol at 37 °C for 2 h to completely detach all carbohydrate ligands from the surface of the AuNPs.[75] After separation from AuNP residues by centrifugal filtration, the samples were concentrated under high vacuum to remove 2-mercaptoethanol and then subjected to the coupled glucoamylase–glucose oxidase/peroxidase assay in 10 mM phosphate buffer pH 7.0 (Figure 3). These results showed that for maltose and maltotriose oxime AuNPs (**11-AuNP** and **12-AuNP**, respectively) the ligand density was around 300 mol ligand/mol AuNPs, when corrected for the release of 2 mol glucose/mol maltotriose oxime. For the oxy-amine AuNPs, however, the ligand density was approximately three times higher, reaching around 1000 mol ligand/mol AuNPs for the maltotriose oxy-amine AuNPs (**15-AuNP**). We hypothesize that this difference in ligand density between oxime glyco-AuNPs and oxy-amine glyco-AuNPs could be due to a steric demand of the dynamic ring-chain tautomerism of glycoconjugates **10**–**12** relative to the open-chain glycoconjugates **13**–**15**.

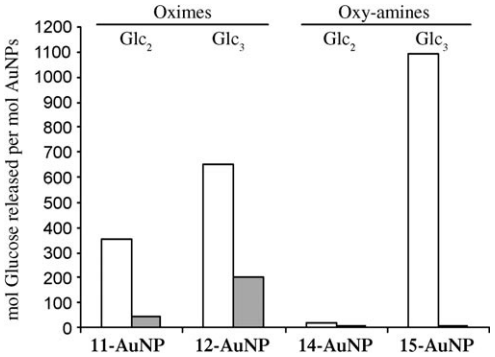

Figure 3. Measurements of release of glucose by glucoamylase after thiolytic release of OEG glycoconjugates from glyco-AuNPs (white bars) and by glucoamylase on glyco-AuNPs (grey bars). The experiment was performed in 10 mM sodium phosphate pH 7.0 at 42 °C using 50 pmol of each glyco-AuNP. As expected, **14-AuNP** showed no response after thiolytic release (Table 2).

Functional recognition of glyco-AuNPs by glucoamylase: Finally, we applied the coupled assay based on glucoamylase (GA) and glucose oxidase/peroxidase, as described above, for estimating the accessibility of the glycan ligands at the surface. Taking into account the topology of the barrel-shaped active site, we reasoned that an ability of GA to release glucose from the surface of the glyconanoparticles would be indicative of a high degree of accessibility. At the outset of this study, we noted that Penadés and co-workers previously examined the enzymatic cleavage of galactose from lactose-AuNPs by a β-galactosidase and found only minute activity of the enzyme (<3% cleaved).[21]

Maltose- and maltotriose-containing glyconanoparticles **11-AuNP**, **12-AuNP**, **14-AuNP**, and **15-AuNP** were subjected to the GA-assay conditions (Figure 3). The results showed that the oxime glyco-AuNPs (**11-AuNP** and **12-AuNP**) allowed a certain level of functional recognition by the enzyme, leading to partial hydrolysis of the glyco-AuNPs under these conditions. Conversely, the maltotriose oxy-amine AuNPs (**15-AuNP**) displayed complete stability towards the enzyme. We ascribe this observation to the increased ligand density observed with these glyco-AuNPs, as measured in the thiolytic-release assay above. These results corroborate the increased stability of glycan ligands on glyconanoparticles towards enzymatic degradation and emphasize the ligand density as a pivotal factor for stability.

Conclusion

The highly chemoselective reaction of glycans through their reducing ends with aminooxy groups, via oxime formation, has become an important method in glycobiology. However, it is most often considered that this leaves the monosaccharide at the reducing end in a non-native open-chain form. Here, we describe, firstly, a novel bifunctional linker for anchoring glycans by oxime formation to nanoparticles and, secondly, that the oxime-tautomer forms include ring-closed forms that are correctly recognized by proteins.

Our design of a novel heterobifunctional OEG linker incorporates the following features: 1) an aminooxy group for the chemoselective capture of reducing glycans under mild conditions, 2) a trityl group that can be used as a handle for isolation of the otherwise highly polar glycoconjugates, 3) a mercapto group that upon deprotection provides chemoselective coupling onto the nanoparticle surface, and 4) a tetra(ethylene glycol) chain that provides aqueous solubility to the nanoparticles and prevents unspecific binding with proteins. Using this linker reagent, we obtained glyconanoparticles that were soluble under a wide range of conditions.

In light of the wide use of the oxime formation for attachment of glycans to surfaces, the consequences of the ring-chain tautomerism of carbohydrate oxime ethers during interaction with proteins is of considerable interest. Our results with two model proteins, glucoamylase from *Aspergillus niger* and concanavalin A from *Concanavalia ensiformis*, show that, in both cases, functional recognition of the carbohydrate oximes occurs with the cyclic tautomeric forms, and that the equilibria exist when the carbohydrate oxime ethers are attached to gold-nanoparticle surfaces. This was corroborated by extensive comparison with the corresponding reduced, open-chain forms. We believe this to be an important finding as it allows efficient anchoring of glycans through the reducing end while maintaining a correct presentation of the glycan.

Experimental Section

Materials and analysis: All chemicals, as well as enzymes and lectins, were purchased from Sigma–Aldrich Denmark, except for polymer-supported triphenylphosphine (PL-TPP resin, PS-PPh_3), which was a gift from Varian (Polymer Laboratories). MilliQ water was used for all aqueous preparations. All solvent ratios are v/v. ^{1}H, ^{13}C, attached proton test (APT), HSQC, and COSY NMR spectra were recorded by using a Bruker Avance 300 spectrometer with a BBO probe. The chemical shifts are referenced to the residual solvent signal. Assignments were aided by COSY, HSQC, and APT experiments. Mass determination (high-resolution MS, HRMS) was performed by using a Micromass LCT instrument with an ESI probe. UV/Vis spectroscopy was performed by using a Jasco V-650 spectrophotometer. Analytical HPLC was performed by using a Dionex Ultimate 3000 system with Chromeleon 6.80SP3 software; a 2.0-mL min^{-1} linear gradient flow of MeCN-H_2O (0.1% trifluoroacetic acid (TFA)) 1:20→1:0 over 6.5 min was used for separations on a C-18 (Daiso, 10 μm, 200 Å, 250×8 mm OD) column from FEF Chemicals. Transmission electron microscopy (TEM) was recorded by using a Philips CM20 instrument at 200 keV.

Synthesis of OEG linkers

N-*(2-{2-[2-(2-Hydroxyethoxy)ethoxy]ethoxy}ethoxy)-phthalimide* (***1***): Tetra-(ethylene glycol) (0,97 g, 5.0 mmol) was dissolved in dry tetrahydrofuran (80 mL) under argon, followed by addition of PS-PPh_3 (5.07 g, 7.5 mmol, 1.48 mmol g^{-1}) and *N*-hydroxyphthalimide (0.82 g, 5.0 mmol). Under stirring, a solution of diisopropylazodicarboxylate (1.52 g, 7.5 mmol) in dry tetrahydrofuran (20 mL) was added dropwise over 30 min. The mixture was stirred for 4 h and then left unstirred for 16 h at RT. The resin was filtered off on a pad of Celite, and the filtrate was concentrated by rotary evaporation. The residue was purified by filtration on a silica plug by washing extensively with ethyl acetate to provide the desired mono-substituted product as a clear oil (622 mg, 37%). ^{1}H NMR (300 MHz, [D]chloroform): δ=7.88–7.80 (m, 2H; Phth *ortho*), 7.78–7.71 (m, 2H; Phth *meta*), 4.41–4.36 (m, 2H; CH_2ON), 3.89–3.84 (m, 2H; OCH_2CH$_2$ON), 3.74–3.66 (m, 4H), 3.66–3.57 (m, 8H), 2.47 ppm (t, J=6.2 Hz, O*H*); ^{13}C NMR (75 MHz, [D]chloroform): δ=163.4 (C=O), 134.4 (Phth *meta*), 128.9 (Phth *ipso*), 123.5 (Phth *ortho*), 77.2 (*C*H$_2$ON), 72.4 (O*C*H$_2$CH$_2$OH), 70.8, 70.6, 70.4, 70.3, 69.2 (OCH$_2$CH$_2$ON), 61.7 ppm (*C*H$_2$OH); HRMS (ES): m/z: calcd for $C_{16}H_{22}NO_7$: 340.1396 [M+H]$^+$; found: 340.1378.

Recovery of the bis-substituted product provided 429 mg (18%) of *N,N′*-(2,2′-{2,2′-oxybis[ethoxy]}bis{ethoxy})diphthalimide (**bis-1**) as a clear oil. ^{1}H NMR (300 MHz, [D]chloroform): δ=7.86–7.78 (m, 4H; Phth *ortho*), 7.77–7.70 (m, 4H; Phth *meta*), 4.38–4.33 (m, 4H; 2×CH_2ON), 3.86–3.81 (m, 4H; 2×OCH_2CH$_2$ON), 3.62–3.55 (m, 4H; 2×CH_2OCH$_2$CH$_2$ON), 3.53–3.46 ppm (m, 4H; 2×OCH_2CH$_2$OCH$_2$CH$_2$ON); ^{13}C NMR (75 MHz, [D]chloroform): δ=163.4 (C=O), 134.4 (Phth *meta*), 128.9 (Phth *ipso*), 123.4 (Phth *ortho*), 77.2 (*C*H$_2$ON), 70.7 (OCH$_2$*C*H$_2$OCH$_2$CH$_2$ON), 70.4 (OCH$_2$CH$_2$OCH$_2$CH$_2$ON), 69.2 ppm (OCH$_2$CH$_2$ON); HRMS (ES): m/z: calcd for $C_{24}H_{25}N_2O_9S$: 485.1560 [M+H]$^+$; found: 485.1572.

N-*(2-{2-[2-(2-Tritylsulfanylethoxy)ethoxy]ethoxy}ethoxy)phthalimide* (***2***): Diisopropylazodicarboxylate (0.607 g, 3.0 mmol) was added to a stirred suspension of polymer-supported triphenylphosphine (2.03 g, 3.0 mmol, 1.48 mmol g^{-1}) in dry tetrahydrofuran (25 mL) at 0°C under argon. The mixture was stirred for 30 min at 0°C. Then, a solution of **1** (0.509 g, 1.5 mmol) and triphenylmethanethiol (0.829 g, 3.0 mmol) in dry tetrahydrofuran (20 mL) was added dropwise at 0°C. The suspension was left to reach RT and stirred for an additional 4 h at RT. The resin was filtered off on a pad of Celite, and the filtrate was concentrated by rotary evaporation. The residue was purified by vacuum liquid chromatography (VLC) (diethylether/heptane 1:1→1:0) to provide the title compound as a clear oil (699 mg, 78%). ^{1}H NMR (300 MHz, [D]chloroform): δ=7.86–7.79 (m, 2H; o-ArH), 7.76–7.69 (m, 2H; m-ArH), 7.44–7.38 (m, 6H; Tr), 7.31–7.16 (m, 9H; Tr), 4.38–4.33 (m, 2H; CH_2ON), 3.87–3.81 (m, 2H; OCH_2CH$_2$ON), 3.66–3.60 (m, 2H), 3.57–3.51 (m, 2H), 3.51–3.45 (m, 2H), 3.43–3.36 (m, 2H), 3.28 (t, J=6.7 Hz, 2H; OCH_2CH$_2$STr), 2.41 ppm (t, J=6.7 Hz, 2H; CH_2STr); ^{13}C NMR (75 MHz, [D]chloroform): δ=163.3 (C=O), 144.7 (Tr ipso), 134.3 (Phth *meta*), 129.5 (Tr), 129.0 (Phth *ipso*), 127.8 (Tr), 126.6 (Tr *para*), 123.4 (Phth *ortho*), 77.1 (*C*H$_2$ON), 70.7, 70.4, 70.3, 70.0, 69.5, 69.2 (OCH$_2$CH$_2$STr), 66.5 (Tr quaternary), 31.6 ppm (*C*H$_2$STr); HRMS (ES): m/z: calcd for $C_{35}H_{36}NO_6$: 620.2083 [M→Na]$^+$; found: 620.2089.

O-*(2-{2-[2-(2-Tritylsulfanylethoxy)ethoxy]ethoxy}ethyl)hydroxylamine* (***3***): Compound **2** (0.598 g, 1.0 mmol) was dissolved in acetonitrile (20 mL) and hydrazine hydrate (230 μL, 5.0 mmol) was added. Stirring for 2 h at RT yielded a white suspension that was concentrated by rotary evaporation. The residue was suspended in dichloromethane and filtered through a plug of Celite. Evaporation to dryness of the filtrate yielded the title compound as a clear oil (0.454 g, 97%). ^{1}H NMR (300 MHz, [D]chloroform): δ=7.44–7.38 (m, 6H; Tr), 7.31–7.16 (m, 9H; Tr), 5.48 (br s, 2H; ONH_2), 3.84–3.79 (m, 2H; CH_2ON), 3.69–3.64 (m, 2H; OCH_2CH$_2$ON), 3.63 (s, 4H), 3.60–3.55 (m, 2H), 3.48–3.43 (m, 2H), 3.31 (t, J=6.9 Hz, 2H; OCH_2CH$_2$STr), 2.43 ppm (t, J=6.9 Hz, 2H; CH_2STr); ^{13}C NMR (75 MHz, [D]chloroform): δ=144.8 (Tr *ipso*), 129.6 (Tr), 127.8 (Tr), 126.6 (Tr *para*), 74.8 (*C*H$_2$ON), 70.6, 70.5, 70.4, 70.1, 69.7, 69.6, 66.6 (Tr quaternary), 31.6 ppm (*C*H$_2$STr); HRMS (ES): m/z: calcd for $C_{27}H_{34}NO_4S$: 468.2209 [M+H]$^+$; found: 468.2199.

General procedure for oxime formation of 3 with glucose, maltose, and maltotriose: The aminooxy linker **3** (150 mg, 0.32 mmol) was dissolved in acetonitrile (5 mL) and either D-glucose, D-maltose monohydrate, or D-maltotriose (0.35 mmol) was added. Water (2–5 mL) was added to provide clear solutions, followed by addition of glacial acetic acid (150 μL). The reaction mixtures were stirred at RT for 16 h and then concentrated by rotary evaporation. The residues were purified by VLC (methanol/dichloromethane 1:20→1:8) to provide the glucose oxime **4** (100 mg, 74%), the maltose oxime **5** (214 mg, 86%), and the maltotriose oxime **6** (270 mg, 88%), respectively, as thick, clear oils.

D-*Glucose* O-*(2-{2-[2-(2-tritylsulfanylethoxy)ethoxy]ethoxy}ethyl)oxime* (***4***): ^{1}H NMR (300 MHz, [D$_4$]methanol, (*E*)-oxime/(*Z*)-oxime/β-pyranose tautomeric ratio 60:20:20): $\delta = 7.44$ (d, $J = 6.7$ Hz, 0.6H; (*E*)-oxime H-1), 7.42–7.36 (m, 6H; Tr), 7.33–7.17 (m, 9H; Tr), 6.78 (d, $J = 6.0$ Hz, 0.2H; (*Z*)-oxime H-1), 4.94 (t, $J = 6.0$ Hz, 0.2H (partly overlapped by H_2O signal); (*Z*)-oxime H-2), 4.32 (t, $J = 6.7$ Hz, 0.6H; (*E*)-oxime H-2), 4.21–4.12 (m, 2.2H; CH_2ON + β-pyranose H-1 ($J = 9.2$ Hz from HSQC)), 3.94–3.85 (m, 0.8H; (*E*)-oxime + (*Z*)-oxime H-3), 3.84–3.18 (m, 16.4H), 2.39 ppm (t, $J = 6.7$ Hz, 2H; CH_2STr); ^{13}C NMR (75 MHz, APT, [D$_4$]methanol): $\delta = 154.2$ ((*Z*)-oxime C-1), 151.8 ((*E*)-oxime C-1), 146.3 (Tr *ipso*), 130.8 (Tr), 129.0 (Tr), 127.8 (Tr), 92.9 (β-pyranose C-1), 79.4, 79.1 (β-pyranose H-2), 74.9 (*C*H$_2$ON), 74.4 (*C*H$_2$ON), 74.1 (*C*H$_2$ON), 73.2, 72.9, 72.7, 72.6, 72.3, 72.2, 72.0, 71.6 (*C*H$_2$ OEG), 71.6 (*C*H$_2$ OEG), 71.4(*C*H$_2$ OEG), 71.2 (*C*H$_2$ OEG), 70.6 (*C*H$_2$ OEG), 70.6 (*C*H$_2$ OEG), 68.5, 67.8 (Tr quarternary), 64.9 (C-6), 63.0 (C-6), 32.8 ppm (*C*H$_2$STr); HRMS (ES): *m*/*z*: calcd for $C_{33}H_{43}NO_9NaS$: 652.2556 $[M+Na]^+$; found: 652.2552.

D-*Maltose* O-*(2-{2-[2-(2-tritylsulfanylethoxy)ethoxy]ethoxy}ethyl)oxime* (***5***): ^{1}H NMR (300 MHz, [D$_4$]methanol, (*E*)-oxime/(*Z*)-oxime/β-pyranose tautomeric ratio 60:20:20): $\delta = 7.49$ (d, $J = 6.7$ Hz, 0.6H; (*E*)-oxime H-1), 7.43–7.36 (m, 6H; Tr), 7.32–7.18 (m, 9H; Tr), 6.83 (d, $J = 5.4$ Hz, 0.2H; (*Z*)-oxime H-1), 5.16 (d, $J = 3.8$ Hz, 0.2H; β-pyranose H-1′), 5.05 (d, $J = 3.9$ Hz, 0.8H; (*E*)-oxime + (*Z*)-oxime H-1′), 4.91 (dd, $J = 5.4$, 2.5 Hz, 0.2H (partly overlapped by H_2O signal); (*Z*)-oxime H-2), 4.43 (dd, $J = 6.7$, 4.3 Hz, 0.6H; (*E*)-oxime H-2), 4.20–4.11 (m, 2.2H; CH_2ON + β-pyranose H-1 ($J = 9.1$ Hz from HSQC)), 4.08–3.22 (m, 23.2H), 2.39 ppm (t, $J = 6.7$ Hz, 2H; CH_2STr); ^{13}C NMR (75 MHz, APT, [D$_4$]methanol): $\delta = 154.8$ ((*Z*)-oxime C-1), 152.1 ((*E*)-oxime C-1), 146.2 (Tr *ipso*), 130.8 (Tr), 128.9 (Tr), 127.8 (Tr), 102.9 (C-1′), 102.7 (C-1′), 102.4 (C-1′), 92.7 (β-pyranose C-1), 84.5, 83.0, 81.2, 78.7, 77.9, 75.1, 75.0, 74.8 (*C*H$_2$ON), 74.7, 74.5, 74.4, 74.1 (*C*H$_2$ON), 74.1, 73.9, 73.8, 73.1, 71.5 (*C*H$_2$ OEG), 71.5 (*C*H$_2$ OEG), 71.5 (*C*H$_2$ OEG), 71.4 (*C*H$_2$ OEG), 71.2 (*C*H$_2$ OEG), 71.1, 70.9, 70.6 (*C*H$_2$ OEG), 70.6 (*C*H$_2$ OEG), 70.4 70.6 (*C*H$_2$ OEG), 67.7 (Tr quarternary), 67.0, 64.0 (C-6), 63.9 (C-6), 62.7 (C-6), 62.6 (C-6), 62.4 (C-6), 32.8 ppm (*C*H$_2$STr); HRMS (ES): *m*/*z*: calcd for $C_{39}H_{53}NO_{14}NaS$: 814.3084 $[M+Na]^+$; found: 814.3090.

D-*Maltotriose* O-*(2-{2-[2-(2-tritylsulfanylethoxy)ethoxy]ethoxy}ethyl)oxime* (***6***): ^{1}H NMR (300 MHz, [D$_4$]methanol, (*E*)-oxime/(*Z*)-oxime/β-pyranose tautomeric ratio 60:20:20): $\delta = 7.49$ (d, $J = 6.7$ Hz, 0.6H; (*E*)-oxime H-1), 7.43–7.36 (m, 6H; Tr), 7.32–7.17 (m, 9H; Tr), 6.84 (d, $J = 5.4$ Hz, 0.2H; (*Z*)-oxime H-1), 5.18 (d, $J = 3.8$ Hz, 1H; H-1″), 5.16 (d, $J = 3.8$ Hz, 0.2H; β-pyranose H-1′), 5.08 (d, $J = 3.9$ Hz, 0.8H; (*E*)-oxime + (*Z*)-oxime H-1′), 4.91 (dd, $J = 5.3$, 2.4 Hz, 0.2H (partly overlapped by H_2O signal); (*Z*)-oxime H-2), 4.43 (dd, $J = 6.6$, 4.3 Hz, 0.6H; (*E*)-oxime H-2), 4.20–4.12 (m, 2.2H; CH_2ON + β-pyranose H-1 ($J = 9.2$ Hz from HSQC)), 4.08–3.22 (m, 29.2H), 2.38 ppm (t, $J = 6.7$ Hz, 2H; CH_2STr); ^{13}C NMR (75 MHz, APT, [D$_4$]methanol): $\delta = 154.8$ ((*Z*)-oxime C-1), 152.1 ((*E*)-oxime C-1), 146.2 (Tr *ipso*), 130.7 (Tr), 128.9 (Tr), 127.8 (Tr), 102.8 (C-1″), 102.7 (C-1″), 102.4 (C-1′), 102.2 (C-1′), 92.7 (β-pyranose C-1), 84.2, 82.9, 81.2, 78.7, 77.8, 75.0, 74.9, 74.8, 74.7, 74.4 (*C*H$_2$ON), 74.3, 74.2 (*C*H$_2$ON), 74.1, 74.1, 73.9, 73.7, 73.4, 73.3, 73.0, 71.6 (*C*H$_2$ OEG), 71.5 (*C*H$_2$ OEG), 71.4, 71.3 (*C*H$_2$ OEG), 71.1 (*C*H$_2$ OEG), 71.0, 70.9, 70.6 (*C*H$_2$ OEG), 70.6 (*C*H$_2$ OEG), 70.3, 70.2, 67.7 (Tr quarternary), 67.1, 64.0 (C-6), 63.9 (C-6), 62.7 (C-6), 62.4 (C-6), 62.0 (C-6), 32.8 ppm (*C*H$_2$STr); HRMS (ES): *m*/*z*: calcd for $C_{45}H_{63}NO_{19}NaS$: 976.3613 $[M+Na]^+$; found: 976.3559.

General procedure for reduction of carbohydrate oximes 4–6: The carbohydrate oximes **4**, **5**, or **6** (0.10 mmol) were dissolved in glacial acetic acid (2 mL) and sodium cyanoborohydride (13 mg, 0.20 mmol) was added. The mixtures were stirred for 2 h at RT and then concentrated by rotary evaporation. The residues were redissolved in methanol and purified on cation-exchange cartridges (Varian Bond Elut SCX) to provide the glucose-derived oxy-amine **7** (58 mg, 92%), the maltose-derived oxy-amine **8** (67 mg, 85%), and the maltotriose-derived oxy-amine **9** (82 mg, 86%) as thick, clear oils.

1-Deoxy-1-(2-{2-[2-(2-tritylsulfanylethoxy)ethoxy]ethoxy}ethoxyamino)-D-*glucitol* (***7***): ^{1}H NMR (300 MHz, [D$_4$]methanol): $\delta = 7.43$–7.37 (m, 6H; Tr), 7.32–7.18 (m, 9H; Tr), 3.99 (ddd, $J = 8.0$, 4.1, 3.9 Hz, 1H; H-2), 3.83–3.75 (m, 4H; CH_2ON, H-3, H-6), 3.70 (dd, $J = 8.6$, 3.1 Hz, 1H; H-4), 3.66–3.58 (m, 8H; 3 × CH_2 OEG, H-5, H-6), 3.57–3.52 (m, 2H; CH_2 OEG), 3.45–3.40 (m, 2H; CH_2 OEG), 3.26 (t, $J = 6.7$ Hz, 2H; OCH_2CH$_2$STr), 3.12 (dd, $J = 13.3$, 3.9 Hz, 1H; H-1), 2.92 (dd, $J = 13.3$, 8.0 Hz, 1H; H-1), 2.39 ppm (t, $J = 6.7$ Hz, 2H; CH_2STr); ^{13}C NMR (75 MHz, APT, [D$_4$]methanol): $\delta = 146.3$ (Tr *ipso*), 130.8 (Tr), 128.9 (Tr), 127.8 (Tr), 73.7 (C-5), 73.6 (*C*H$_2$ON), 73.0 (C-4), 72.1 (C-3), 71.5 (*C*H$_2$ OEG), 71.5 (*C*H$_2$ OEG), 71.4 (C-2), 71.4 (*C*H$_2$ OEG), 71.2 (*C*H$_2$ OEG), 70.6 (*C*H$_2$ OEG), 70.6 (*C*H$_2$ OEG), 67.8 (Tr quarternary), 64.8 (C-6), 55.2 (C-1), 32.8 ppm (*C*H$_2$STr); HRMS (ES): *m*/*z*: calcd for $C_{33}H_{45}NO_9NaS$: 654.2713 $[M+Na]^+$; found: 654.2664.

1-Deoxy-1-(2-{2-[2-(2-tritylsulfanylethoxy)ethoxy]ethoxy}ethoxyamino)-D-*maltitol* (***8***): ^{1}H NMR (300 MHz, [D$_4$]methanol): $\delta = 7.43$–7.37 (m, 6H; Tr), 7.32–7.18 (m, 9H; Tr), 5.03 (d, $J = 4.0$ Hz, 1H; H-1′), 4.00 (ddd, $J = 8.0$, 4.4, 2.0 Hz, 1H; H-2), 3.94–3.59 (m, 17H), 3.58–3.52 (m, 2H; CH_2 OEG), 3.49–3.40 (m, 3H; CH_2 OEG, C-4′), 3.34–3.28 (m, 1H; overlapped by [D$_4$]methanol peak), 3.27 (t, $J = 6.7$ Hz, 2H; OCH_2CH$_2$STr), 3.05 (dd, $J = 13.5$, 4.4 Hz, 1H; H-1), 3.00 (dd, $J = 13.5$, 8.0 Hz, 1H; H-1), 2.39 ppm (t, $J = 6.7$ Hz, 2H; CH_2STr); ^{13}C NMR (75 MHz, APT, [D$_4$]methanol): $\delta = 146.3$ (Tr *ipso*), 130.8 (Tr), 128.9 (Tr), 127.8 (Tr), 102.9 (C-1′), 85.5 (C-5′), 75.1, 74.5, 74.2, 73.8, 73.7 (*C*H$_2$ON), 73.4, 71.6 (*C*H$_2$ OEG), 71.5, 71.5 (*C*H$_2$ OEG), 71.4 (*C*H$_2$ OEG), 71.2 (*C*H$_2$ OEG), 70.6 (*C*H$_2$ OEG), 70.6 (*C*H$_2$ OEG), 69.2, 67.8 (Tr quarternary), 64.0 (C-6), 62.6 (C-6), 55.8 (C-1), 32.8 ppm (*C*H$_2$STr); HRMS (ES): *m*/*z*: calcd for $C_{39}H_{55}NO_{14}NaS$: 816.3241 $[M+Na]^+$; found: 814.3232.

1-Deoxy-1-(2-{2-[2-(2-tritylsulfanylethoxy)ethoxy]ethoxy}ethoxyamino)-D-*maltotritol* (***9***): ^{1}H NMR (300 MHz, [D$_4$]methanol): $\delta = 7.43$–7.37 (m, 6H; Tr), 7.32–7.18 (m, 9H; Tr), 5.18 (d, $J = 3.8$ Hz, 1H; H-1″), 5.04 (d, $J = 3.9$ Hz, 1H; H-1′), 4.00 (ddd, $J = 7.8$, 4.4, 1.9 Hz, 1H; H-2), 3.96–3.24 (m, 31H), 3.07 (dd, $J = 13.5$, 4.4 Hz, 1H; H-1), 2.98 (dd, $J = 13.5$, 7.8 Hz, 1H; H-1), 2.39 ppm (t, $J = 6.7$ Hz, 2H; CH_2STr); ^{13}C NMR (75 MHz, APT, [D$_4$]methanol): $\delta = 146.2$ (Tr *ipso*), 130.8 (Tr), 128.9 (Tr), 127.8 (Tr), 102.8 (C-1″), 102.7 (C-1′), 85.2, 81.3, 75.1, 74.9, 74.7, 74.2, 74.2, 73.7 (*C*H$_2$ON), 73.4, 73.3, 73.0, 71.6 (*C*H$_2$ OEG), 71.5, 71.5 ((*C*H$_2$ OEG), 71.4 (*C*H$_2$ OEG), 71.2 (*C*H$_2$ OEG), 70.7 (*C*H$_2$ OEG), 70.6 (*C*H$_2$ OEG), 69.2, 67.8 (Tr quarternary), 64.0 (C-6), 62.7 (C-6), 62.1 (C-6), 55.8 (C-1), 32.8 ppm (*C*H$_2$STr); HRMS (ES): *m*/*z*: calcd for $C_{45}H_{65}NO_{19}NaS$: 978.3769 $[M+Na]^+$; found: 978.3701.

General procedure for removal of the trityl group from compounds 4–9: Compounds **4**, **5**, **6**, **7**, **8**, or **9** (0.050 mmol) were dissolved/suspended in dichloromethane (1 mL) under argon. Triethylsilane (0.5 mL) was added, followed by a dropwise addition of trifluoroacetic acid (1 mL) under stirring. A transient yellow color was observed during the addition, however, all reaction mixtures were clear solutions after the addition. The reaction mixtures were stirred at RT for 5 min and then concentrated by rotary evaporation. The residues were purified by redissolution in methanol/dichloromethane 1:20–1:10 and filtration through a silica plug. Once washed, the plug was thoroughly dried and the products were then eluted by methanol. Evaporation to dryness provided the desired thiols **10**–**15** as thick, clear oils in quantitative yields, partially as disulfides (0–40%).

D-*Glucose* O-*(2-{2-[2-(2-mercaptoethoxy)ethoxy]ethoxy}ethyl)oxime* (***10***): ^{1}H NMR (300 MHz, [D$_4$]methanol, (*E*)-oxime/(*Z*)-oxime/β-pyranose tautomeric ratio 60:20:20, 25% disulfide): $\delta = 7.45$ (d, $J = 6.9$ Hz, 0.6H; (*E*)-oxime H-1), 6.79 (d, $J = 6.1$ Hz, 0.2H; (*Z*)-oxime H-1), 4.94 (dd, $J = 6.1$, 5.4 Hz, 0.2H (partly overlapped by H_2O signal); (*Z*)-oxime H-2), 4.32 (dd, $J = 6.9$, 6.3 Hz, 0.6H; (*E*)-oxime H-2), 4.23–4.15 (m, 2.2H; CH_2ON + β-pyranose H-1), 3.92 (dd, $J = 5.4$, 2.1 Hz, 0.2H; (*Z*)-oxime H3), 3.88 (dd, $J = 6.3$, 1.6 Hz, 0.8H; (*E*)-oxime H-3), 3.84–3.00 (m, 16.4H), 2.92 (t, $J =$

6.4 Hz, 0.5H; CH_2S disulfide), 2.66 ppm (t, J=6.5 Hz, 1.5H; CH_2SH); ^{13}C NMR (75 MHz, APT, [D$_4$]methanol, 25% disulfide): δ=154.2 ((*Z*)-oxime C-1), 151.8 ((*E*)-oxime C-1), 92.8 (β-pyranose C-1), 86.9 (OCH_2CH$_2$S disulfide), 79.4, 79.1, 74.9 (CH_2ON), 74.4 (CH_2ON), 74.2 (CH_2ON), 74.1 (OCH_2CH$_2$SH) 73.2, 72.9, 72.7, 72.6, 72.3, 72.2, 72.0, 92.7, 71.6 (CH_2 OEG), 71.5 (CH_2 OEG), 71.3, CH_2 OEG), 71.1 (CH_2 OEG), 70.6 (CH_2 OEG), 70.5 (CH_2 OEG), 70.5 (CH_2 OEG), 68.5, 64.9 (C-6), 63.0 (C-6), 39.5 (CH_2S disulfide), 24.7 ppm (CH_2SH); HRMS (ES): *m*/*z*: calcd for $C_{14}H_{30}NO_9S$: 388.1641 [*M*+H]$^+$; found: 388.1666.

D-*Maltose* O-*(2-{2-[2-(2-mercaptoethoxy)ethoxy]ethoxy}ethyl)oxime* (***11***): ^{1}H NMR (300 MHz, [D$_4$]methanol, (*E*)-oxime/(*Z*)-oxime/β-pyranose tautomeric ratio 60:20:20, 40% disulfide): δ=7.50 (d, J=6.5 Hz, 0.6H; (*E*)-oxime H-1), 6.84 (d, J=5.4 Hz, 0.2H; (*Z*)-oxime H-1), 5.16 (d, J=3.6 Hz, 0.2H; β-pyranose H-1′), 5.05 (d, J=3.8 Hz, 0.8H; (*E*)-oxime+(*Z*)-oxime H-1′), 4.91 (m, 0.2H (partly overlapped by H_2O signal); (*Z*)-oxime H-2), 4.44 (dd, J=6.5, 4.2 Hz, 0.6H; (*E*)-oxime H-2), 4.24–4.15 (m, 2.2H; CH_2ON+β-pyranose H-1), 4.08–3.00 (m, 23.2H), 2.92 (t, J=6.4 Hz, 0.8H; CH_2S disulfide), 2.66 ppm (t, J=6.4 Hz, 1.2H; CH_2STr); ^{13}C NMR (75 MHz, APT, [D$_4$]methanol, 40% disulfide): δ=154.8 ((*Z*)-oxime C-1), 152.1 ((*E*)-oxime C-1), 146.2 (Tr *ipso*), 130.8 (Tr), 128.9 (Tr), 127.8 (Tr), 102.9 (C-1′), 102.7 (C-1′), 102.4 (C-1′), 92.7 (β-pyranose C-1), 86.9 (OCH_2CH$_2$S disulfide), 84.5, 83.0, 81.2, 78.7, 77.9, 75.1, 75.0, 74.8 (CH_2ON), 74.7, 74.5, 74.4, 74.1 (CH_2ON), 74.1, 73.9, 73.8, 73.1, 71.6 (CH_2 OEG), 71.5 (CH_2 OEG), 71.4 (CH_2 OEG), 71.3 (CH_2 OEG), 71.1 (CH_2 OEG), 70.9, 70.7 (CH_2 OEG), 70.6 (CH_2 OEG), 70.5 (CH_2 OEG), 70.3 (CH_2 OEG), 67.0, 64.0 (C-6), 63.9 (C-6), 62.7 (C-6), 62.6 (C-6), 62.4 (C-6), 39.5 (CH_2S disulfide), 24.6 ppm (CH_2SH); HRMS (ES): *m*/*z*: calcd for $C_{20}H_{40}NO_{14}S$: 550.2170 [*M*+H]$^+$; found: 550.2194.

D-*Maltotriose* O-*(2-{2-[2-(2-mercaptoethoxy)ethoxy]ethoxy}ethyl)oxime* (***12***): ^{1}H NMR (300 MHz, [D$_4$]methanol, (*E*)-oxime/(*Z*)-oxime/β-pyranose tautomeric ratio 60:20:20, 30% disulfide): δ=7.50 (d, J=6.3 Hz, 0.6H; (*E*)-oxime H-1), 6.86 (d, J=5.3 Hz, 0.2H; (*Z*)-oxime H-1), 5.19–5.15 (m, 1.2H; H-1″, β-pyranose H-1′), 5.13–5.08 (m, 0.8H; (*E*)-oxime+(*Z*)-oxime H-1′), 4.94–4.90 (m, 0.2H (partly overlapped by H_2O signal); (*Z*)-oxime H-2), 4.46 (dd, J=6.2, 3.9 Hz, 0.6H; (*E*)-oxime H-2), 4.24–4.16 (m, 2.2H; CH_2ON+β-pyranose H-1), 4.14–2.98 (m, 29.2H), 2.92 (t, J=6.4 Hz, 0.6H; CH_2S disulfide), 2.67 ppm (t, J=6.4 Hz, 1.4H; CH_2STr); ^{13}C NMR (75 MHz, APT, [D$_4$]methanol): δ=154.8 ((*Z*)-oxime C-1), 152.1 ((*E*)-oxime C-1), 102.8 (C-1″), 102.7 (C-1″), 102.4 (C-1′), 102.2 (C-1′), 92.7 (β-pyranose C-1), 84.2, 82.9, 81.2, 78.7, 77.8, 75.0, 74.9, 74.8, 74.7, 74.4 (CH_2ON), 74.3, 74.2 (CH_2ON), 74.1, 74.1, 73.9, 73.7, 73.4, 73.2, 71.5 (CH_2 OEG), 71.4 (CH_2 OEG), 71.3 (CH_2 OEG), 71.2 (CH_2 OEG), 71.2, 71.1 (CH_2 OEG), 71.0 (CH_2 OEG), 70.7 (CH_2 OEG), 70.6 (CH_2 OEG), 70.4 (CH_2 OEG), 67.7, 64.0 (C-6), 63.9 (C-6), 62.7 (C-6), 62.4 (C-6), 62.0 (C-6), 39.4 (CH_2S disulfide), 24.6 ppm (CH_2SH); HRMS (ES): *m*/*z*: calcd for $C_{26}H_{50}NO_{19}S$: 712.2698 [*M*+H]$^+$; found: 712.2717.

1-Deoxy-1-(2-{2-[2-(2-mercaptoethoxy)ethoxy]ethoxy}ethoxyamino)-D-*glucitol* (***13***): ^{1}H NMR (300 MHz, [D$_4$]methanol, 0% disulfide): δ=4.00 (ddd, J=8.0, 4.1, 3.9 Hz, 1H; H-2), 3.86–3.79 (m, 3H; CH_2ON and H-3), 3.78–3.61 (m, 14H), 3.61 (t, J=6.5 Hz, 2H; OCH_2CH$_2$SH), 3.12 (dd, J=13.3, 3.9 Hz, 1H; H-1), 3.11 (dd, J=13.3, 8.0 Hz, 1H; H-1), 2.66 ppm (t, J=6.7 Hz, 2H; CH_2SH); ^{13}C NMR (75 MHz, APT, [D$_4$]methanol, 0% disulfide): δ=74.1 (OCH_2CH$_2$SH), 74.1, 73.7 (CH_2ON), 73.0, 71.7, 71.6, 71.5 (CH_2 OEG), 71.5 (CH_2 OEG), 71.4 (CH_2 OEG), 71.1 (CH_2 OEG), 70.7 (CH_2 OEG), 64.7 (C-6), 55.3 (C-1), 24.6 ppm (CH_2SH); HRMS (ES): *m*/*z*: calcd for $C_{14}H_{32}NO_9S$: 390.1798 [*M*+H]$^+$; found: 390.1804.

1-Deoxy-1-(2-{2-[2-(2-mercaptoethoxy)ethoxy]ethoxy}ethoxyamino)-D-*maltitol* (***14***): ^{1}H NMR (300 MHz, [D$_4$]methanol, 15% disulfide): δ=5.07 (d, J=4.0 Hz, 1H; H-1′), 4.03 (ddd, J=7.8, 4.6, 1.4 Hz, 1H; H-2), 4.00–3.62 (m, 21H), 3.61 (t, J=6.5 Hz, 2H; OCH_2CH$_2$SH), 3.50 (dd, J=9.7, 4.0 Hz, 1H; C-4′), 3.34–3.27 (m, 1H; overlapped by [D$_4$]methanol peak), 3.08 (dd, J=13.5, 4.6 Hz, 1H; H-1), 2.99 (dd, J=13.5, 7.8 Hz, 1H; H-1), 2.92 (t, J=6.5 Hz, 0.3H; CH_2S disulfide), 2.67 ppm (t, J=6.5 Hz, 1.7H; CH_2SH); ^{13}C NMR (75 MHz, APT, [D$_4$]methanol): δ=102.6 (C-1′), 84.7 (C-5′), 74.9, 74.7, 74.3, 74.1 (OCH_2CH$_2$SH), 73.7, 73.7 (CH_2ON), 72.6, 71.5 (CH_2 OEG), 71.4 (CH_2 OEG), 71.4 (CH_2 OEG), 71.3, 71.1 (CH_2 OEG), 70.7 (CH_2 OEG), 70.4, 69.8, 63.9 (C-6), 62.6 (C-6), 55.8 (C-1), 39.4 ((CH_2S disulfide), 24.6 ppm (CH_2SH); HRMS (ES): *m*/*z*: calcd for $C_{20}H_{42}NO_{14}S$: 552.2326 [*M*+H]$^+$; found: 552.2367.

1-Deoxy-1-(2-{2-[2-(2-mercaptoethoxy)ethoxy]ethoxy}ethoxyamino)-D-*maltotritol* (***15***): ^{1}H NMR (300 MHz, [D$_4$]methanol, 10% disulfide): δ=5.17 (d, J=3.8 Hz, 1H; H-1″), 5.07 (d, J=3.9 Hz, 1H; H-1′), 4.02 (m, 1H; H-2), 3.99–3.23 (m, 31H), 3.08 (dd, J=13.5, 4.5 Hz, 1H; H-1), 2.99 (dd, J=13.5, 7.8 Hz, 1H; H-1), 2.93 (t, J=6.4 Hz, 0.2H; CH_2S disulfide), 2.67 ppm (t, J=6.5 Hz, 1.8H; CH_2SH); ^{13}C NMR (75 MHz, APT, [D$_4$]methanol): δ=102.9 (C-1″), 102.5 (C-1′), 84.8, 81.3, 75.1, 74.8, 74.8, 74.3, 74.2, 74.1 (OCH_2CH$_2$SH), 73.7 (CH_2ON), 73.3, 73.1, 72.8, 71.5 (CH_2 OEG), 71.4 (CH_2 OEG), 71.4 (CH_2 OEG) 71.3, 71.1 (CH_2 OEG), 70.7 (CH_2 OEG), 70.4, 69.7, 64.0 (C-6), 62.7 (C-6), 62.0 (C-6), 55.7 (C-1), 39.4 (CH_2S disulfide), 24.6 ppm (CH_2SH); HRMS (ES): *m*/*z*: calcd for $C_{26}H_{52}NO_{19}S$: 714.2854 [*M*+H]$^+$; found: 714.2916.

NMR study: D-[1-^{13}C]Glucose ***O***-**(2-{2-[2-(2-tritylsulfanylethoxy)ethoxy]-ethoxy}-ethyl)oxime (16)**: The aminooxy linker **3** (23 mg, 0.050 mmol) was dissolved in acetonitrile (2 mL) and D-[1-^{13}C]glucose (14 mg, 0.075 mmol) was added. Water (1 mL) was added, followed by glacial acetic acid (50 μL). The reaction mixtures were stirred at RT for 16 h and then concentrated by rotary evaporation. The residue was purified by VLC (methanol/dichloromethane 1:20→1:6) to provide the [1-^{13}C]glucose oxime **16** (22 mg, 70% as a clear, thick oil. ^{1}H NMR (300 MHz, [D$_4$]methanol, (*E*)-oxime/(*Z*)-oxime/β-pyranose tautomeric ratio 60:20:20): δ=7.44 (dd, J=6.9, 166.4 Hz, 0.6H; (*E*)-oxime H-1), 7.42–7.36 (m, 6H; Tr), 7.33–7.17 (m, 9H; Tr), 6.78 (dd, J=6.1, 178.2 Hz, 0.2H; (*Z*)-oxime H-1), 4.94 (dt, J=4.3, 6.1 Hz, 0.2H (partly overlapped by H_2O signal); (*Z*)-oxime H-2), 4.32 (dt, J=4.7, 6.9 Hz, 0.6H; (*E*)-oxime H-2), 4.21–4.12 (m, 2.2H; CH_2ON+β-pyranose H-1 (J=9.0, 152.9 Hz from H;H-COSY)), 3.94–3.85 (m, 0.8H; (*E*)-oxime+(*Z*)-oxime H-3), 3.84–3.18 (m, 16.4H), 2.39 ppm (t, J=6.7 Hz, 2H; CH_2STr); ^{13}C NMR (75 MHz, APT, [D$_4$]methanol): δ=154.2 ((*Z*)-oxime ^{13}C-1), 151.8 ((*E*)-oxime ^{13}C-1), 146.3 (Tr *ipso*), 130.8 (Tr), 129.0 (Tr), 127.8 (Tr), 95.6 (minor), 92.9 (β-pyranose ^{13}C-1), 90.7 (minor), 79.4, 79.1, 74.9 (CH_2ON), 74.4 (CH_2ON), 74.1 (CH_2ON), 73.2, 72.9, 72.7, 72.6, 72.3, 72.2, 72.0, 71.6 (CH_2 OEG), 71.6 (CH_2 OEG), 71.4(CH_2 OEG), 71.2 (CH_2 OEG), 70.6 (CH_2 OEG), 70.6 (CH_2 OEG), 68.5, 67.8 (Tr quarternary), 64.9 (C-6), 63.0 (C-6), 32.8 ppm (CH_2STr); HRMS (ES): *m*/*z*: calcd for $C_{32}H_{43}NO_9S^{13}C$: 653.2589 [*M*+Na]$^+$; found: 653.2670.

Preparation of 12-nm diameter citrate-stabilized gold nanoparticles: Spherical citrate-stabilized gold nanoparticles were prepared by the Turkevich protocol[19] according to a recently published procedure.[69] Briefly, a warm (≈50–60 °C) solution of sodium citrate dihydrate (228 mg, 0.776 mmol) in helium-degassed MilliQ water (20 mL) was added to a stirred solution of hydrogen tetrachloroaurate(III) trihydrate (79 mg, 0.200 mmol) in helium-degassed MilliQ water (200 mL) at reflux. The resulting dark-red solution was stirred at reflux for 30 min, where after it was cooled to RT and filtered through a 0.25 μm syringe filter.

Ligand exchange and purification of gold glyconanoparticles: Solutions of **10**, **11**, **12**, **13**, **14**, or **15** (0.050 mmol) in methanol (5 mL) were added to stirred solutions of citrate-stabilized gold nanoparticles (50 mL). A slight color change towards purple was observable. The solutions were stirred for a minimum of 16 h and the gold glyconanoparticles were purified in 10-mL batches by centrifugal filtration (Millipore Amicon Centriplus 50 kDa) with five consecutive filtration and redissolution (2 mL MilliQ water, 10× dilution) steps. After the final filtration, the gold glyconanoparticles were redissolved in 10 mM phosphate buffer pH 7.0 (400 μL) to provide final nanoparticle concentrations of 0.50 μM of **10-AuNP**, **11-AuNP**, **12-AuNP**, **13-AuNP**, **14-AuNP**, and **15-AuNP**.

Glucoamylase assays: Glucoamylase (GA)-catalyzed hydrolysis in solution (50 μL in 1.5-mL centrifuge tubes) was performed using 1 mg mL^{-1} GA in 10 mM sodium phosphate pH 7.0 at 42 °C with 10 nmol of either the free saccharides D-glucose, D-maltose monohydrate, and D-maltotriose or compounds **4**, **5**, **6**, **7**, **8**, and **9**, respectively, as substrate. Released glucose was measured after 20 h by using the glucose oxidase–peroxidase assay kit (Sigma–Aldrich), with reaction volumes adapted for use in microplates and microplate reader (PowerWave$_x$, Bio-Tek Instruments), measuring the absorbance at 540 nm.

Adaptation of the assay for the use on glyconanoparticles (50 pmol particles) required inclusion of a centrifugal filtration step (Amicon Ultrafree-MC 30 kDa cut-off from Millipore) immediately after hydrolysis to remove gold nanoparticles that would otherwise interfere with absorption measurements at 540 nm.

Thiolytic quantification of ligands on AuNPs: Glyconanoparticles (50 μL, 0.5 μM) were treated with 2-mercaptoethanol (50 μL, 1.0 M in water) at 37 °C for 2 h. The resulting dark suspensions were filtered through microfiltration cartridges (Amicon Ultrafree-MC 30 kDa cut-off from Millipore) to remove gold nanoparticles, and the filtrates were concentrated by freeze drying. Remaining 2-mercaptoethanol was removed under high vacuum at 80 °C for 4 h. The completely odorless residues were redissolved in 10 mM phosphate buffer pH 7.0 (50 μL). GA-catalyzed hydrolysis was performed on the samples with measurement of released glucose by using the glucose oxidase–peroxidase assay kit, as described above.

Lectin assay: Aqueous dispersions of glyconanoparticles (5 nM) were treated with a final concentration of 5.0 μM of concanavalin A from *Concanavalia ensiformis* by addition of a 1.25 mg mL^{-1} solution in water. Aggregation was monitored by UV/Vis spectroscopy by measurement of the shifts in surface-plasmon peak maximum over a period of 48 h.

Acknowledgements

The authors kindly thank Inger Jensen at the Nano-Science Center at the University of Copenhagen for transmission electron microscopy (TEM) measurements on gold glyconanoparticles. We also thank Dr. Andrew Coffey from Varian Inc. (Polymer Laboratories) for the polymer-supported triphenylphosphine (PL-TPP resin) and Stig Jacobsen for HRMS determinations. FNU is gratefully acknowledged for a grant (K.J.J.). Finally, Dr. Emiliano Cló is gratefully acknowledged for help with preparation of this manuscript.

[1] A. Varki, *Glycobiology* **1993**, *3*, 97–130.
[2] T. Feizi, *Glycoconjugate J.* **2000**, *17*, 553–565.
[3] K. M. Koeller, C. H. Wong, *Nat. Biotechnol.* **2000**, *18*, 835–841.
[4] For a review, see: K. Larsen, M. B. Thygesen, F. Guillaumie, W. G. T. Willats, K. J. Jensen, *Carbohydr. Res.* **2006**, *341*, 1209–1234.
[5] F. Guillaumie, J. D. Sterling, K. J. Jensen, O. R. T. Thomas, D. Mohnen, *Carbohydr. Res.* **2003**, *338*, 1951–1960.
[6] F. Guillaumie, S. F. L. Justesen, K. E. Mutenda, P. Roepstorff, K. J. Jensen, O. R. T. Thomas, *Carbohydr. Res.* **2006**, *341*, 118–129.
[7] S. I. Nishimura, K. Niikura, M. Kurogochi, T. Matsushita, M. Fumoto, H. Hinou, R. Kamitani, H. Nakagawa, K. Deguchi, N. Miura, K. Monde, H. Kondo, *Angew. Chem.* **2005**, *117*, 93–98; *Angew. Chem. Int. Ed.* **2005**, *44*, 91–96.
[8] M. Lee, I. Shin, *Org. Lett.* **2005**, *7*, 4269–4272.
[9] O. Bohorov, H. Andersson-Sand, J. Hoffmann, O. Blixt, *Glycobiology* **2006**, *16*, 21C–27C.
[10] Y. Liu, T. Feizi, M. A. Campanero-Rhodes, R. A. Childs, Y. Zhang, B. Mulloy, P. G. Evans, H. M. I. Osborn, D. Otto, P. R. Crocker, W. Chai, *Chem. Biol.* **2007**, *14*, 847–859.
[11] S. E. Cervigni, P. Dumy, M. Mutter, *Angew. Chem.* **1996**, *108*, 1325–1328; *Angew. Chem. Int. Ed. Engl.* **1996**, *35*, 1230–1232.
[12] A. Lohse, R. Martins, M. R. Jorgensen, O. Hindsgaul, *Angew. Chem.* **2006**, *118*, 4273–4278; *Angew. Chem. Int. Ed.* **2006**, *45*, 4167–4172.
[13] F. Guillaumie, O. R. T. Thomas, K. J. Jensen, *Bioconjugate Chem.* **2002**, *13*, 285–294.
[14] S. Hanson, M. Best, M. C. Bryan, C. H. Wong, *Trends Biochem. Sci.* **2004**, *29*, 656–663.
[15] O. Blixt, K. Allin, L. Pereira, A. Datta, J. C. Paulson, *J. Am. Chem. Soc.* **2002**, *124*, 5739–5746.
[16] J. M. De la Fuente, S. Penades, *Biochim. Biophys. Acta Gen. Subj.* **2006**, *1760*, 636–651.
[17] A. G. Barrientos, J. M. de la Fuente, T. C. Rojas, A. Fernandez, S. Penades, *Chem. Eur. J.* **2003**, *9*, 1909–1921.
[18] M. Brust, M. Walker, D. Bethell, D. J. Schiffrin, R. Whyman, *J. Chem. Soc. Chem. Commun.* **1994**, 801–802.
[19] J. Turkevich, P. C. Stevenson, J. Hillier, *J. Phys. Chem.* **1953**, *57*, 670–673.
[20] G. Frens, *Nature Phys. Sci.* **1973**, *241*, 20–22.
[21] J. M. de la Fuente, A. G. Barrientos, T. C. Rojas, J. Rojo, J. Canada, A. Fernandez, S. Penades, *Angew. Chem.* **2001**, *113*, 2317–2321; *Angew. Chem. Int. Ed.* **2001**, *40*, 2257–2261.
[22] K. M. Halkes, A. C. de Souza, C. E. P. Maljaars, G. J. Gerwig, J. P. Kamerling, *Eur. J. Org. Chem.* **2005**, 3650–3659.
[23] A. Sundgren, J. J. Barchi, Jr., *Carbohydr. Res.* **2008**, *343*, 1594–1604.
[24] D. C. Hone, A. H. Haines, D. A. Russell, *Langmuir* **2003**, *19*, 7141–7144.
[25] C. C. Lin, Y. C. Yeh, C. Y. Yang, G. F. Chen, Y. C. Chen, Y. C. Wu, C. C. Chen, *Chem. Commun.* **2003**, 2920–2921.
[26] S. A. Svarovsky, Z. Szekely, J. J. Barchi, *Tetrahedron: Asymmetry* **2005**, *16*, 587–598.
[27] R. J. Baues, G. R. Gray, *J. Biol. Chem.* **1977**, *252*, 57–60.
[28] F. Peri, P. Dumy, M. Mutter, *Tetrahedron* **1998**, *54*, 12269–12278.
[29] R. E. Valters, W. Flitsch, *Ring-Chain Tautomerism*, Plenum Press, New York, **1985**.
[30] P. Finch, Z. Merchant, *J. Chem. Soc. Perkin Trans. 1* **1975**, 1682–1686.
[31] Y. Hatanaka, U. Kempin, P. Jong-Jip, *J. Org. Chem.* **2000**, *65*, 5639–5643.
[32] S. L. Ramsay, C. Freeman, P. B. Grace, J. W. Redmond, J. K. MacLeod, *Carbohydr. Res.* **2001**, *333*, 59–71.
[33] C. Delgado, G. E. Francis, D. Fisher, *Crit. Rev. Ther. Drug Carrier Syst.* **1992**, *9*, 249–304.
[34] R. B. Greenwald, Y. H. Choe, J. McGuire, C. D. Conover, *Adv. Drug Delivery Rev.* **2003**, *55*, 217–250.
[35] C. Pale-Grosdemange, E. S. Simon, K. L. Prime, G. M. Whitesides, *J. Am. Chem. Soc.* **1991**, *113*, 12–20.
[36] A. G. Kanaras, F. S. Kamounah, K. Schaumburg, C. J. Kiely, M. Brust, *Chem. Commun.* **2002**, 2294–2295.
[37] F. Zhang, M. W. A. Skoda, R. M. J. Jacobs, S. Zorn, R. A. Martin, C. M. Martin, G. F. Clark, G. Goerigk, F. Schreiber, *J. Phys. Chem. A* **2007**, *111*, 12229–12237.
[38] E. E. Foos, A. W. Snow, M. E. Twigg, M. G. Ancona, *Chem. Mater.* **2002**, *14*, 2401–2408.
[39] W. P. Wuelfing, S. M. Gross, D. T. Miles, R. W. Murray, *J. Am. Chem. Soc.* **1998**, *120*, 12696–12697.
[40] M. Zheng, Z. G. Li, X. Y. Huang, *Langmuir* **2004**, *20*, 4226–4235.
[41] M. Zheng, F. Davidson, X. Y. Huang, *J. Am. Chem. Soc.* **2003**, *125*, 7790–7791.
[42] A. Badia, L. Cuccia, L. Demers, F. Morin, R. B. Lennox, *J. Am. Chem. Soc.* **1997**, *119*, 2682–2692.
[43] J. J. Li, X. G. Peng, *J. Nanosci. Nanotechnol.* **2004**, *4*, 565–568.
[44] S. Jin, C. V. Miduturu, D. C. McKinney, S. K. Silverman, *J. Org. Chem.* **2005**, *70*, 4284–4299.
[45] B. Bendiak, *Carbohydr. Res.* **1997**, *304*, 85–90.
[46] K. Hiromi, Z. I. Hamauzu, K. Takahash, S. Ono, *J. Biochem.* **1966**, *59*, 411–418.
[47] K. Hiromi, K. Takahash, Z. I. Hamauzu, S. Ono, *J. Biochem.* **1966**, *59*, 469–475.
[48] P. J. Reilly, *Starch/Staerke* **1999**, *51*, 269–274.
[49] J. Sauer, B. W. Sigurskjold, U. Christensen, T. P. Frandsen, E. Mirgorodskaya, M. Harrison, P. Roepstorff, B. Svensson, *Biochim. Biophys. Acta Protein Struct. Mol. Enzymol.* **2000**, *1543*, 275–293.
[50] E. Boel, M. T. Hansen, I. Hjort, I. Hoegh, N. P. Fiil, *EMBO J.* **1984**, *3*, 1581–1585.
[51] J. H. Nunberg, J. H. Meade, G. Cole, F. C. Lawyer, P. McCabe, V. Schweickart, R. Tal, V. P. Wittman, J. E. Flatgaard, M. A. Innis, *Mol. Cell. Biol.* **1984**, *4*, 2306–2315.
[52] T. P. Frandsen, C. Dupont, J. Lehmbeck, B. Stoffer, M. R. Sierks, R. B. Honzatko, B. Svensson, *Biochemistry* **1994**, *33*, 13808–13816.
[53] A. E. Aleshin, B. Stoffer, L. M. Firsov, B. Svensson, R. B. Honzatko, *Biochemistry* **1996**, *35*, 8319–8328.

[54] M. R. Sierks, C. Ford, P. J. Reilly, B. Svensson, *Protein Eng.* **1990**, *3*, 193–198.
[55] E. M. S. Harris, A. E. Aleshin, L. M. Firsov, R. B. Honzatko, *Biochemistry* **1993**, *32*, 1618–1626.
[56] A. E. Aleshin, L. M. Firsov, R. B. Honzatko, *J. Biol. Chem.* **1994**, *269*, 15631–15639.
[57] A. E. Aleshin, C. Hoffman, L. M. Firsov, R. B. Honzatko, *J. Mol. Biol.* **1994**, *238*, 575–591.
[58] B. Svensson, A. J. Clarke, I. Svendsen, H. Moller, *Eur. J. Biochem.* **1990**, *188*, 29–38.
[59] K. Hiromi, M. Ohnishi, A. Tanaka, *Mol. Cell. Biochem.* **1983**, *51*, 79–95.
[60] M. M. Meagher, Z. L. Nikolov, P. J. Reilly, *Biotechnol. Bioeng.* **1989**, *34*, 681–688.
[61] M. R. Sierks, C. Ford, P. J. Reilly, B. Svensson, *Protein Eng.* **1989**, *2*, 621–625.
[62] S. Natarajan, M. R. Sierks, *Biochemistry* **1996**, *35*, 3050–3058.
[63] M. R. Sierks, B. Svensson, *Protein Eng.* **1994**, *7*, 1479–1484.
[64] M. R. Sierks, B. Svensson, *Protein Eng.* **1992**, *5*, 185–188.
[65] T. P. Frandsen, T. Christensen, B. Stoffer, J. Lehmbeck, C. Dupont, R. B. Honzatko, B. Svensson, *Biochemistry* **1995**, *34*, 10162–10169.
[66] L. M. Firsov, K. N. Neustroev, A. E. Aleshin, C. M. Metzler, D. E. Metzler, R. D. Scott, B. Stoffer, T. Christensen, B. Svensson, *Eur. J. Biochem.* **1994**, *223*, 293–302.
[67] S. Günther, H. Heymann, *Arch. Biochem. Biophys.* **1998**, *354*, 111–116.
[68] A. Cogoli, G. Semenza, *J. Biol. Chem.* **1975**, *250*, 7802–7809.
[69] R. Levy, N. T. K. Thanh, R. C. Doty, I. Hussain, R. J. Nichols, D. J. Schiffrin, M. Brust, D. G. Fernig, *J. Am. Chem. Soc.* **2004**, *126*, 10076–10084.
[70] W. Haiss, N. T. K. Thanh, J. Aveyard, D. G. Fernig, *Anal. Chem.* **2007**, *79*, 4215–4221.
[71] T. C. Bissot, R. W. Parry, D. H. Campbell, *J. Am. Chem. Soc.* **1957**, *79*, 796–800.
[72] I. J. Goldstein, C. E. Hollerman, E. E. Smith, *Biochemistry* **1965**, *4*, 876–883.
[73] I. J. Goldstein, R. N. Iyer, E. E. Smith, L. L. So, *Biochemistry* **1967**, *6*, 2373–2377.
[74] C. F. Brewer, R. D. Brown, *Biochemistry* **1979**, *18*, 2555–2562.
[75] L. M. Demers, C. A. Mirkin, R. C. Mucic, R. A. Reynolds, R. L. Letsinger, R. Elghanian, G. Viswanadham, *Anal. Chem.* **2000**, *72*, 5535–5541.

Received: July 25, 2008
Revised: October 14, 2008
Published online: December 29, 2008

